Title
MASS TRANSPORT AND POTENTIAL DISTRIBUTION IN THE GEOMETRIES OF LOCALIZED CORROSION

Author
Newman, J.

Publication Date
1987-06-01

Lawrence Berkeley Laboratory
UNIVERSITY OF CALIFORNIA

Materials & Chemical Sciences Division

Presented at the International Conference on Localized Corrosion, Orlando, FL, June 1, 1987

MASS TRANSPORT AND POTENTIAL DISTRIBUTION IN THE GEOMETRIES OF LOCALIZED CORROSION

J. Newman

June 1987

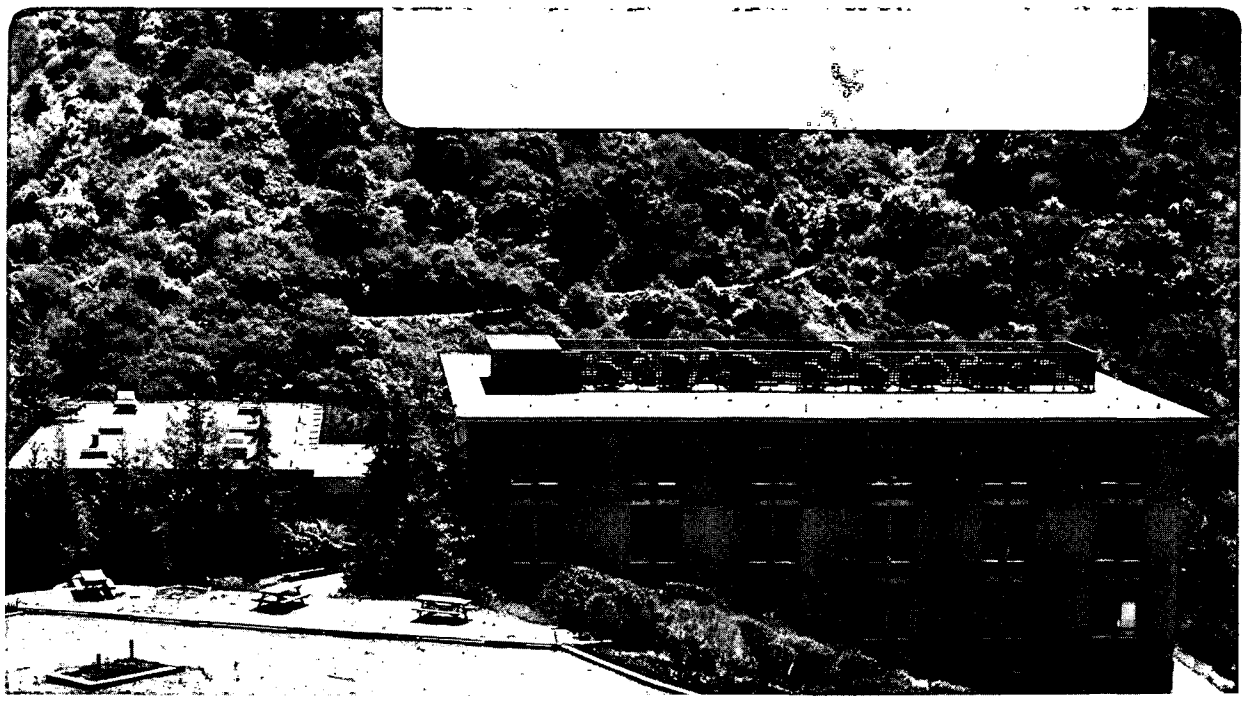

Prepared for the U.S. Department of Energy under Contract DE-AC03-76SF00098

DISCLAIMER

LBL-23474

Mass Transport and Potential Distribution in the Geometries of Localized Corrosion

John Newman

Materials and Chemical Sciences Division,
Lawrence Berkeley Laboratory, and
Department of Chemical Engineering,
University of California,
Berkeley, California 94720

June 24, 1987

Abstract

Localized corrosion, such as pitting, crevice, and water-line corrosion, necessarily involves a passivating metal—one for which an increase in the local electrode potential results in a decrease in the dissolution current. In this situation, the anodic and the cathodic reactions occur in different locations. Consequently, transport of charge and material species in the solution is involved in processes of localized corrosion.

Here fundamental aspects of mass transfer and potential distribution are reviewed with an eye toward applications in localized corrosion. Recent work on passivation, salt-film formation, and oscillatory behavior on iron in 1 M sulfuric acid is reviewed as well as modeling efforts on the partly active, partly passive corrosion of rotating iron disks in sea water.

Key words: Current distribution, salt-film formation, passivation, oscillations.

Introduction

Localized corrosion involves a separation of cathodic and anodic processes, so that anodic dissolution occurs predominantly on one part of a surface and a cathodic process, such as oxygen reduction or hydrogen evolution, occurs predominantly on another. Thus, there must be an electric current flowing in the solution from one part to another. Transport of charge and mass in the solution must be considered in addition to processes occurring directly at the interface.

The purpose of this work is to review briefly the transport processes in solution and the applications of modeling. There are complex and intimate interactions between these transport processes and the interfacial processes of electrochemical reactions, adsorption, and formation of compact and porous films. We want to carry the modeling through toward an enhanced understanding of localized corrosion and of corrosion more generally.

Transport Processes in Electrolytic Solution

In modeling electrolytic solutions, we seek to predict the electric potential and the concentrations of various species as these vary with position and with time. This usually requires us to establish governing partial differential equations and to apply mathematical tools to solve these equations, either analytically or numerically. The transport phenomena involved are complex and generally interact with each other and with processes at the interface between the solution and adjacent metals and insulators.

The fundamental transport relations are discussed in more detail elsewhere,[1,2] including their underlying validity and also approximations useful in applications. A study of those works will give the reader a better feeling for how these governing relations work. Here we shall try to be brief.

Central to the analysis is an equation describing a material balance on each species, specifying how the concentration changes in time in response to transport and chemical reaction.

$$\frac{\partial c_i}{\partial t} = - \nabla \cdot N_i + R_i \quad . \tag{1}$$

This is a bookkeeping equation embodying a reliable physical statement about the conservation or reaction of species. Here, c_i is the concentration of species i, N_i is the flux density of species i, and R_i is the rate of production of species i by homogeneous chemical reactions. To go along with this equation, there must be a transport equation describing how the species moves under the influence of a concentration gradient, an electric field, convective fluid motion, and interaction with other species in the solution. The transport equation can take a relatively simple form, one known for perhaps one hundred years, in which diffusion coefficients are taken to be constant and interactions simple, or it can take a more complicated form valid in concentrated solutions. In dilute solutions, we write

$$N_i = -z_i u_i F c_i \nabla \Phi - D_i \nabla c_i + c_i v \quad , \tag{2}$$

where z_i is the charge number, u_i is the mobility, and D_i is the diffusion coefficient of species i, Φ is the electric potential, F is

Faraday's constant, and v is the fluid velocity.

The current density i in the solution is due to the movement of the charged species:

$$i = F \sum_i z_i N_i \quad . \tag{3}$$

Finally, in order to have enough equations to calculate the electric potential Φ as well as the concentrations, it is necessary to state that the solution is electrically neutral:

$$\sum_i z_i c_i = 0 \quad . \tag{4}$$

For concentrated solutions, such as we expect to find in a corrosion pit or a crevice, we should like to replace the transport equation 2 with the multicomponent diffusion equation[1,2] and also consider the composition dependence of the transport properties. Sometimes we proceed with the dilute-solution equation because it gives approximately the right behavior and we don't know the transport properties well enough to justify the additional complexity of the multicomponent diffusion equation.

Interfacial Processes

The boundary conditions distinguish different situations. The concentration or the normal component of the flux density, or a relationship between them, must be specified on surfaces bounding the solution. Here we want to describe the physics and chemistry as we best understand them. The boundary condition is likely to describe

the kinetics of electron transfer or of adsorption and desorption. We may wish to deal with the formation of salt films or passivating films at the interface. The potential V of a metal is generally uniform, and it is the difference between V and the potential Φ_0 of the solution adjacent to the interface that provides the electric driving force for these interfacial processes.

Frequently charge transfer and adsorption are described by rate expressions with potential dependent rate constants (so-called Butler-Volmer kinetics), but the formation of compact films can modify substantially the basic kinetic laws, as we shall discuss presently.

Current Distributions

Over the decades, the treatment of electrochemical systems according to the model equations presented in the preceding section has proceeded with simplifications and approximations. These have been reviewed in the references previously cited.[1,2]

One limiting case is the situation where there is a lot of supporting electrolyte and the electric field in the solution is reduced to the point where the migration term in equation 2 is negligible. Then we can say that the current distribution is governed by convection and diffusion. To eliminate interactions with the kinetics of interfacial processes, the convective-diffusion situation can be studied at the limiting current, where the electrode potential takes an extreme value so that the concentration of a limiting reactant approaches zero at the surface of the electrode.

The migration term is obviously negligible if the limiting reactant is uncharged, like oxygen, an important corrosion agent. Figure 1 is intended to illustrate a steel piling in the sea, with a substantial flow past it. A simple principle of corrosion says that one should first calculate the limiting rate of transfer of oxygen to the corroding metal. In this case, the limiting rate, expressed as a current density, is sketched in polar coordinates. The rate is high on the front side where the fresh solution impinges on the surface, but it is also high on the back side where there is turbulence and eddy flow to enhance mass transfer.[3] Such an analysis would permit an estimate of the rate of corrosion of the piling. It also is the first step in the design of a system for cathodic protection of the piling. A sample calculation was given in a previous paper.[2] First, one needs to know the distribution of the cathodic reaction. Then one can select the size and placement of anodes so as to provide this protection current, without driving any part of the structure into hydrogen evolution.

This need to know the potential distribution brings us to the opposite extreme in the simplification of the analysis according to the transport equations in the preceding section—namely the neglect of concentration variations altogether. In this case, the equations can be combined to show that the potential in the solution satisfies Laplace's equation. The first simple case usually treated is called the *primary distribution* and involves the assumption that the solution adjacent to an electrode is at a uniform potential—as if electrode

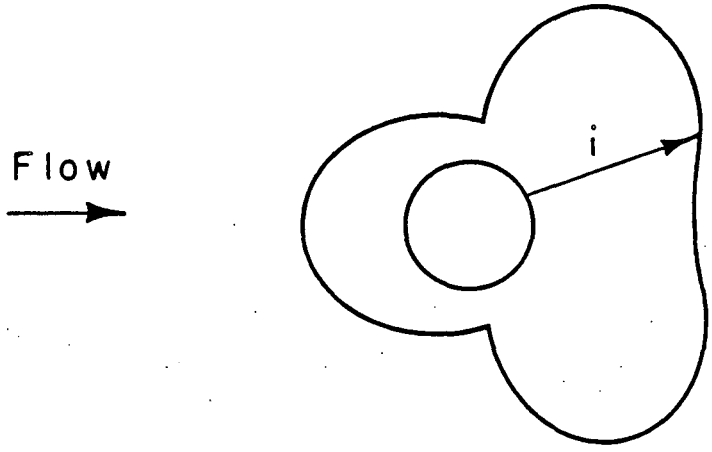

XBL7110-4607

Figure 1. Limiting current distribution around a cylinder at high Reynolds number.

kinetics were very fast and surface overpotentials were negligible.

When electrode overpotentials and kinetics are considered in addition to ohmic potential drop, the situation is known as a *secondary current distribution*. Concentration gradients are still taken to be zero, and Laplace's equation still applies. Problems in which concentration variations are considered, as well as ohmic potential drop and electrode kinetics, are sometimes termed problems of *tertiary current distribution*. We can see how corrosion problems might fall in this classification. Table 1 summarizes these definitions.

While a lot of work has been done on the primary distribution, a little reflection suggests that it is not of compelling interest for corrosion problems. The result is a calculated nonuniform current distribution which is independent of the size of the system. It does not, for example, give any indication of whether a current for cathodic protection will reach all parts of a body. Instead, we may wish to know how large a system can be protected, and for this we need to calculate how the potential varies adjacent to an electrode sur-

Table 1. Current distributions.

Convective-diffusion (limiting current)
Primary (ohmic limited)
Secondary (ohmic and surface kinetics)
Tertiary (all factors simultaneously)

face. We cannot find this if we assume that the potential is zero at the beginning. Some sample calculations of how large a body can be protected have been given in earlier work.[2]

Before going on to complicated problems, let us look at some interesting cases of the solution of Laplace's equation. We seek the potential distribution determined for a situation where the current distribution is prescribed on an electrode surface. Figure 2 shows a pit geometry,[4] where the current density has been taken to be uniform on the pit surface, a condition required for preservation of shape of a growing hemispherical pit. The cathodic reaction may well take place on the surrounding plane, but it is spread over a substantial distance. Consequently, we may take the current density to be zero on the surrounding plane and place the counterelectrode at infinity, where the potential is taken to be zero.

Figure 2 shows current lines (labeled from I = 0 to I = 0.8) and equipotential surfaces, which cross the current lines at right angles. The labels on the current lines denote the fraction of the total current flowing between the line and the axis of symmetry. These lines originate on the pit surface and go off to infinity, not touching the planar surface, which is assumed to be an insulator. Since the pit is not at uniform potential, the equipotential surfaces can intersect this surface as well as the surrounding plane. The plot indicates that the tangential component of the current density in the solution becomes very high at the lip of the pit. One may be particularly interested in the potential values at the lip of the pit and at

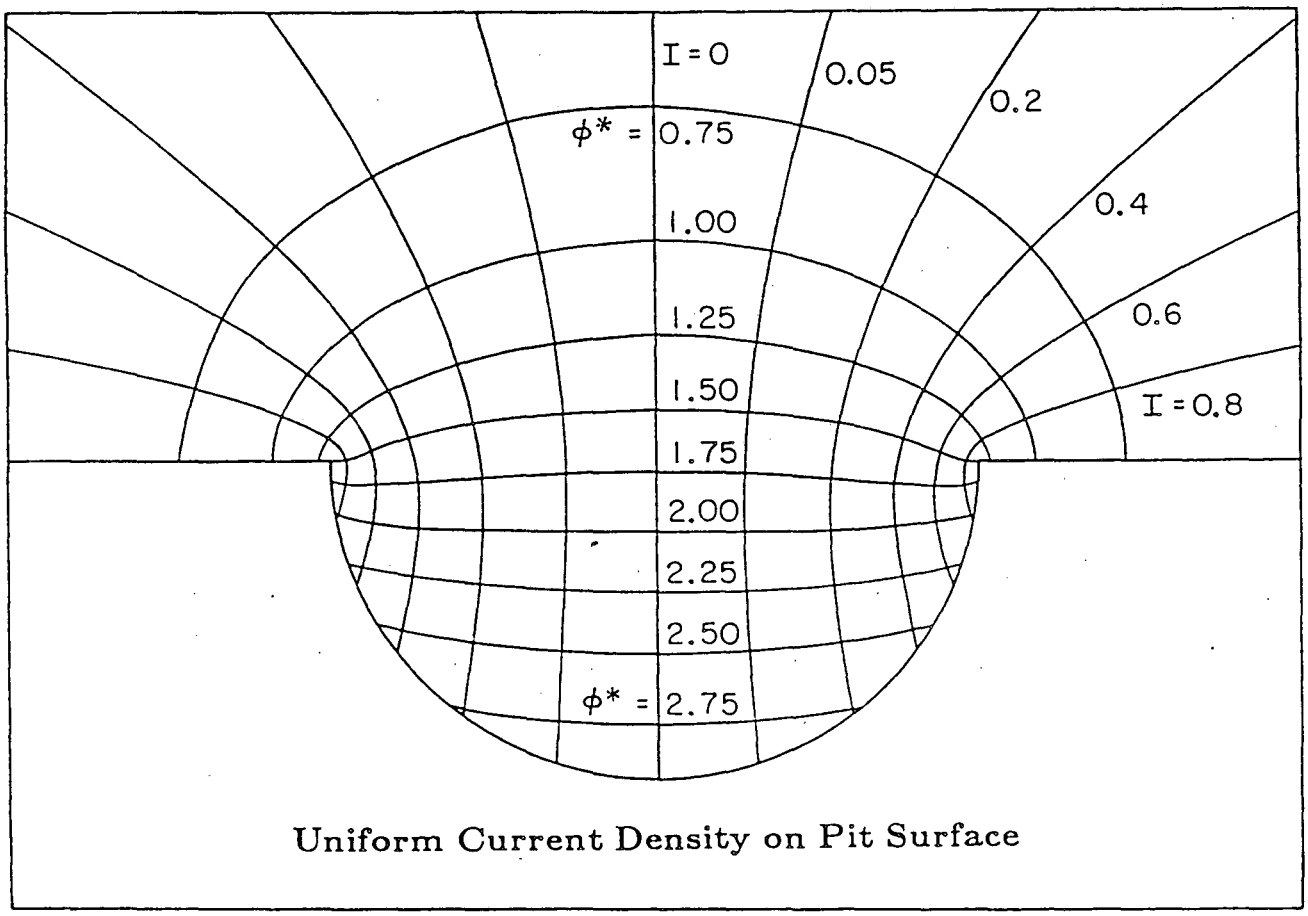

Figure 2. Potential distribution and current lines for a pit, with a uniform current density on the pit surface and a zero current density on the surrounding plane. Values of I indicate the fraction of the current which flows between that curve and the axis of symmetry.

the bottom of the pit because we need to consider the kinetics of the dissolution and passivation processes.

One could also use figure 2 to make estimates of concentration variations. Under steady conditions and with constant physical properties, a species concentration may also obey Laplace's equation, with boundary conditions analogous to those used here.

Table 2 shows the maximum potential difference on the surface in several different geometries. The potential difference in each case is made dimensionless with the average current density on the surface, the radius r_0 of the object, and the electrical conductivity κ of the solution. Comparison of table 2 and figure 2 shows that the value 1.495 is the difference in the values of the dimensionless potential at the lip and the bottom of the pit.

A geometry complementary to the pit is a hemisphere situated on an insulating plane with the counterelectrode at infinity. For a uniform current density, the potential adjacent to the surface would be uniform. Consequently, we have used the limiting current as the basis

Table 2. Maximum potential difference.

geometry	$\frac{\kappa\Delta\Phi}{\langle i\rangle r_0}$	current
disk	0.363	uniform
hemisphere	0.546	limiting
pit	1.495	uniform

for calculating the maximum potential variation.[5]

A disk is intermediate between the hemisphere and the pit, and it is also a geometry of interest in corrosion. Let us assume that we have a disk inclusion with a uniform current density. The maximum potential variation on the disk surface, when made dimensionless, is 0.363 if the surrounding plane is insulating[6] but 0.6366 if the surrounding plane is of uniform potential.[7] Figure 3 shows the current lines and equipotential surfaces for the latter situation. Again, these lines are perpendicular to each other, but this time no equipotential surfaces (except $\Phi = 0$) intersect the surrounding plane, and the current lines are perpendicular to this surface.

Localized Corrosion

Figures 2 and 3 depict possible geometries of localized corrosion, with the region of net anodic current density toward the center of the diagram and the region of net cathodic current density toward the edge. This means that the potential Φ_0 in the solution adjacent to the surface would generally decrease from the center, as sketched in figure 4. On this figure, we have also sketched the potential V of the metal, taken to be uniform because of the high conductivity of the metal. Thus, the potential difference $V - \Phi_0$ will be more positive, or more favoring of anodic processes, toward the periphery, where cathodic processes actually dominate. This can happen only if the rate of anodic dissolution of the metal decreases in some range as this potential difference increases. Figure 5 sketches such a pas-

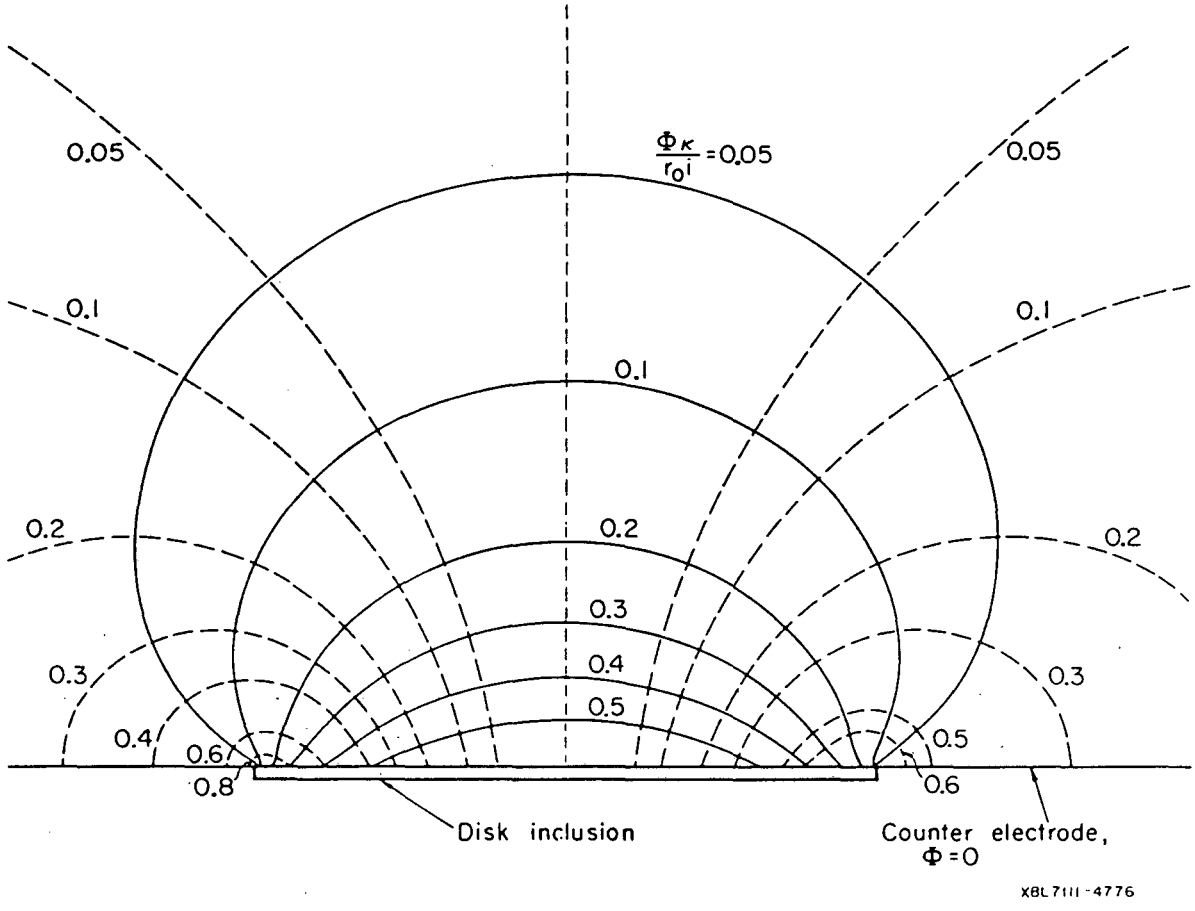

Figure 3. Potential distribution and current lines for a disk inclusion, with a uniform current density and an equipotential plane. Numbers on the dashed curves indicate the fraction of the current which flows between that curve and the axis of symmetry.

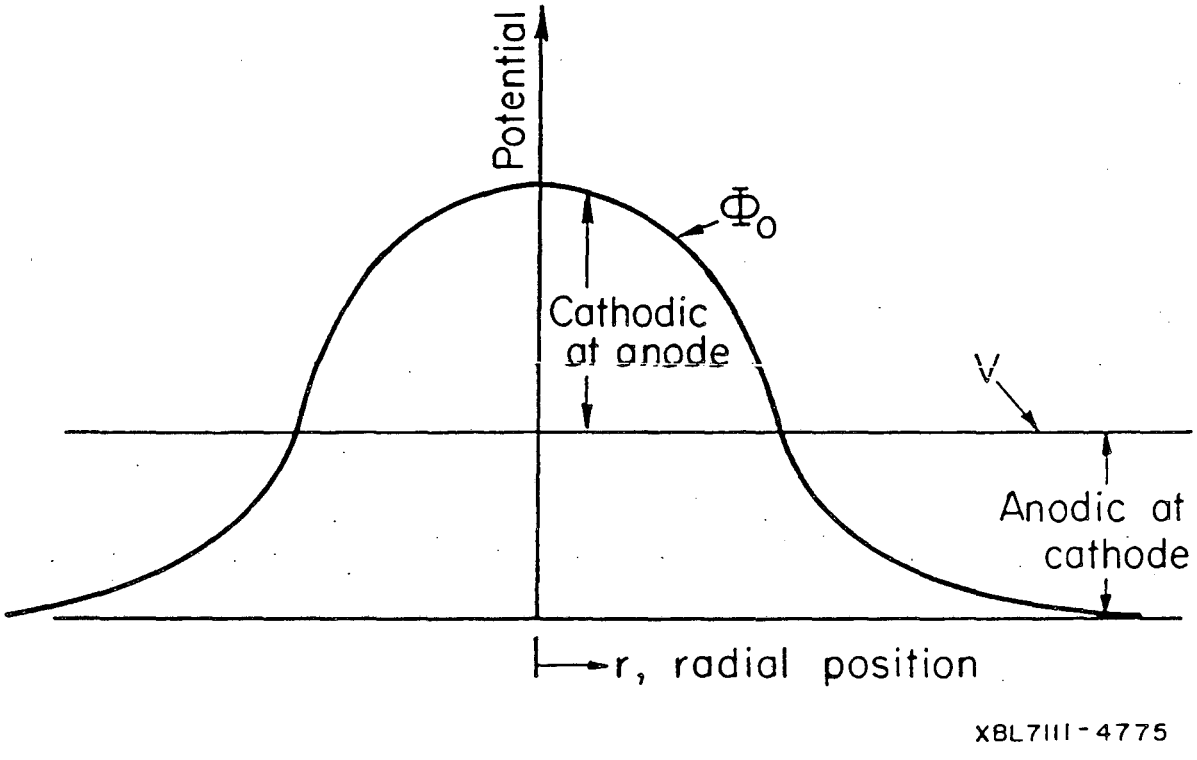

Figure 4. Electrode potential V and adjacent solution potential Φ_0 for a localized corrosion with predominantly anodic behavior in the central region.

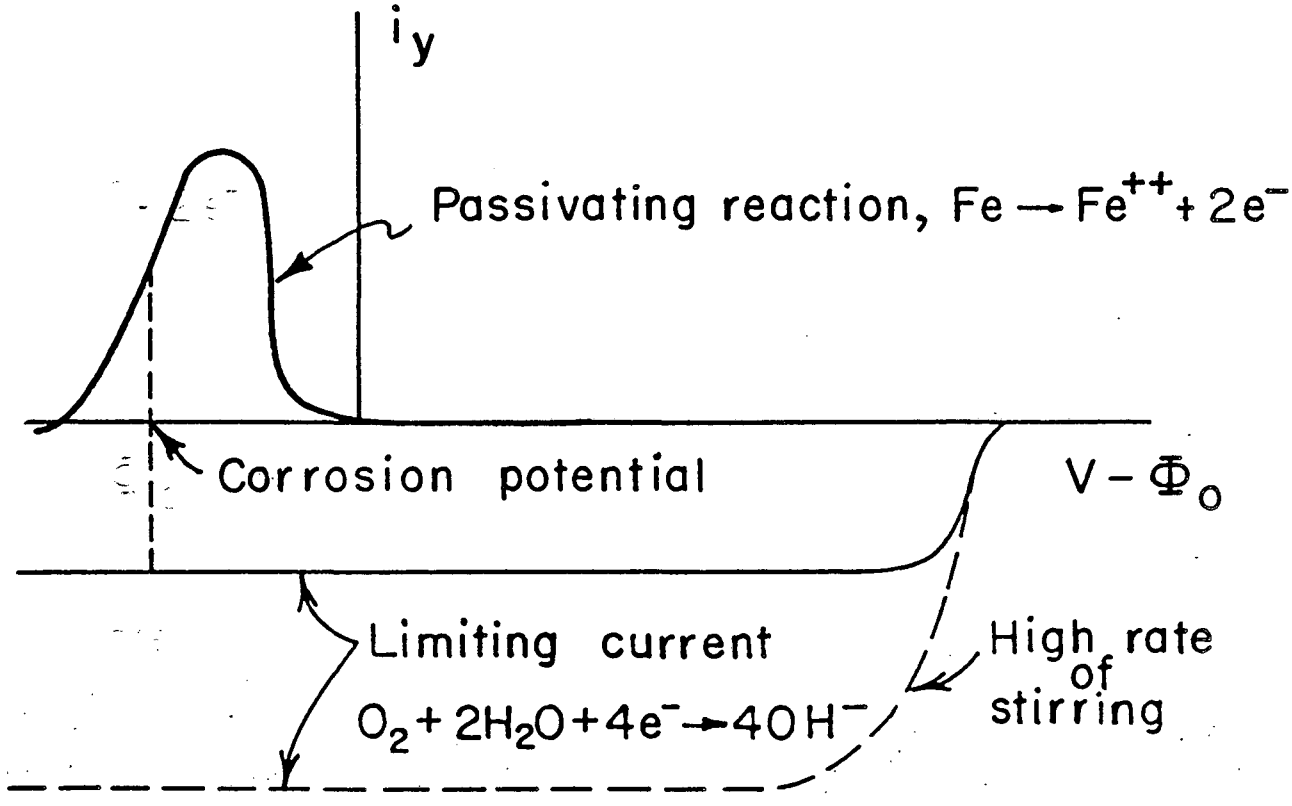

XBL7110-4606

Figure 5. Current-potential behavior of a passivating reaction and of a reaction exhibiting a limiting current, the latter at two rates of stirring.

sivating reaction for iron. Here the normal component i_y of the current density at the surface is plotted against the potential driving force $V - \Phi_0$ for electrochemical reactions. The upper curve shows negative values of i_y at the left, then a zero rate, followed by active dissolution, where the rate rises to a plateau and then drops more or less abruptly as the electrode passivates, or forms a protective oxide film.

For cathodic protection of this iron surface, one seeks to maintain the electrode potential $V - \Phi_0$ toward the left on figure 5 so as to suppress the dissolution reaction. This requires fairly negative potentials and may result in undesirable hydrogen evolution on some parts of the surface. For anodic protection, one seeks to maintain the electrode potential $V - \Phi_0$ toward the right so as to assure that the electrode is passivated. This is easier to accomplish for stainless steels, which are alloyed so as to reduce the maximum rate of dissolution before passivation occurs.

Figure 5 also shows the rate of oxygen reduction for two assumed rates of stirring. The open-circuit potential for the oxygen reaction is quite positive, and oxygen solubility is low. Consequently, the oxygen reaction displays a limiting current density over much of the potential range.

Simple corrosion situations (not localized corrosion) require a local balance of the anodic and cathodic processes. For the solid oxygen curve and the iron curve on figure 5, there are 3 such points; the dashed line at the left indicates one in the active region where

the rate of iron dissolution balances the rate of oxygen reduction. Another balance point occurs toward the right, where the iron is passivated and the oxygen reaction is close to its equilibrium potential. The third balance point is on the descending part of the iron curve and might be expected to be unstable.

For the higher rate of stirring depicted on figure 5, there is only one balance point for the iron and oxygen reactions. At this potential, the iron reaction is passivated, and the rates of both reactions are quite small. Thus, more corrosive conditions such as a higher rate of mass transfer of oxygen can lead to a reduced rate of corrosion if the metal can passivate.

Figure 6 illustrates three concepts of passivation. Curve a, from measured results of Epelboin *et al.*[8,9] after correction for ohmic potential drop, doubles back on itself. For simplicity, Law and Newman[10,11] used a curve (curve b) which drops sharply upon passivation, corresponding to a sharp lip on a pit. On the other hand, El Miligy *et al.*[12] have a model of electrode processes which leads to a gradual decline of the current density with potential in the passivation region (curve c).

Figure 6 also shows a current plateau before passivation. This plateau seems to be mass-transfer limited according to the measurements of Epelboin *et al.*[13] Vetter and Strehblow[14] discussed the possibility of salt films in pitting corrosion, and the concept has been refined by Alkire *et al.*[15] See also the review of Beck.[16]

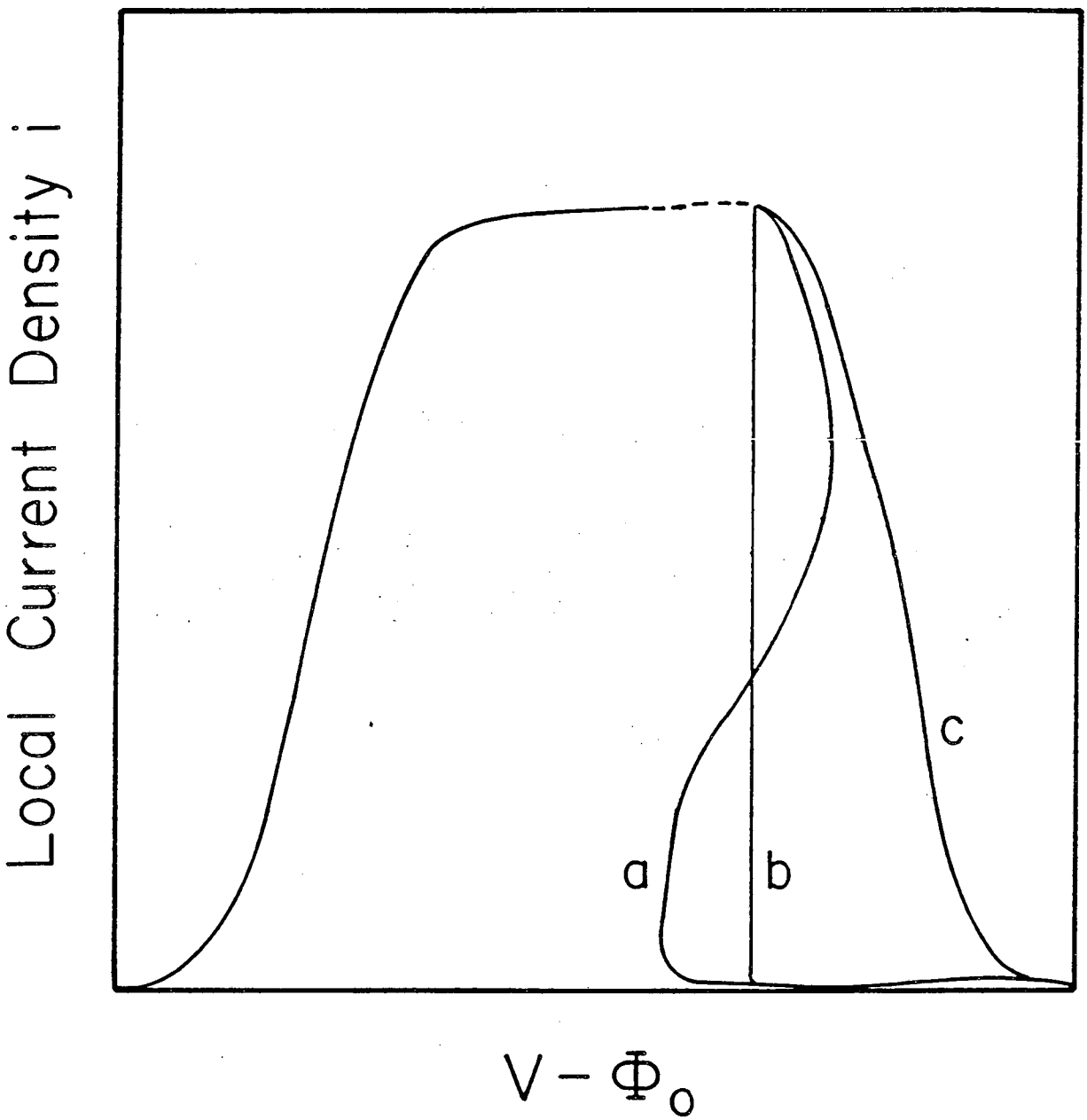

Figure 6. Current-potential plots for three possible modes of passivation.

The potential at which the metal passivates has been called the Flade potential. Pourbaix[17] gave us the plot of this potential as a function of pH (solid line) in figure 7. For contrast, he also depicted the equilibrium line for formation of Fe_2O_3. In order to reach the conditions of potential and pH required for passivation, it may be necessary to form first a slightly porous salt film on the surface, as we shall discuss subsequently.

Iron in 1 M Sulfuric Acid

Iron has been studied extensively in 1 M sulfuric acid in the absence of a corrosive agent like oxygen in order to understand passivation better. We will discuss here a model of salt-film formation in relation to passivation and current oscillations, which are observed with this system.

Figure 8 shows schematically a current-potential curve for iron in 1 M sulfuric acid.[13,18,19] As we sweep from left to right, the current rises during the process of active dissolution of iron. The actual current sweeps through a maximum and a minimum before reaching a plateau; these transients appear to be related to a fast sweep rate[13] or to concentration changes and the formation of a film of ferrous sulfate.[15,20,19] These details, which are not observed on a reverse sweep, have been omitted from figure 8. The film formation presumably leads to a limiting current, proportional to the square root of the rotation speed.[13]

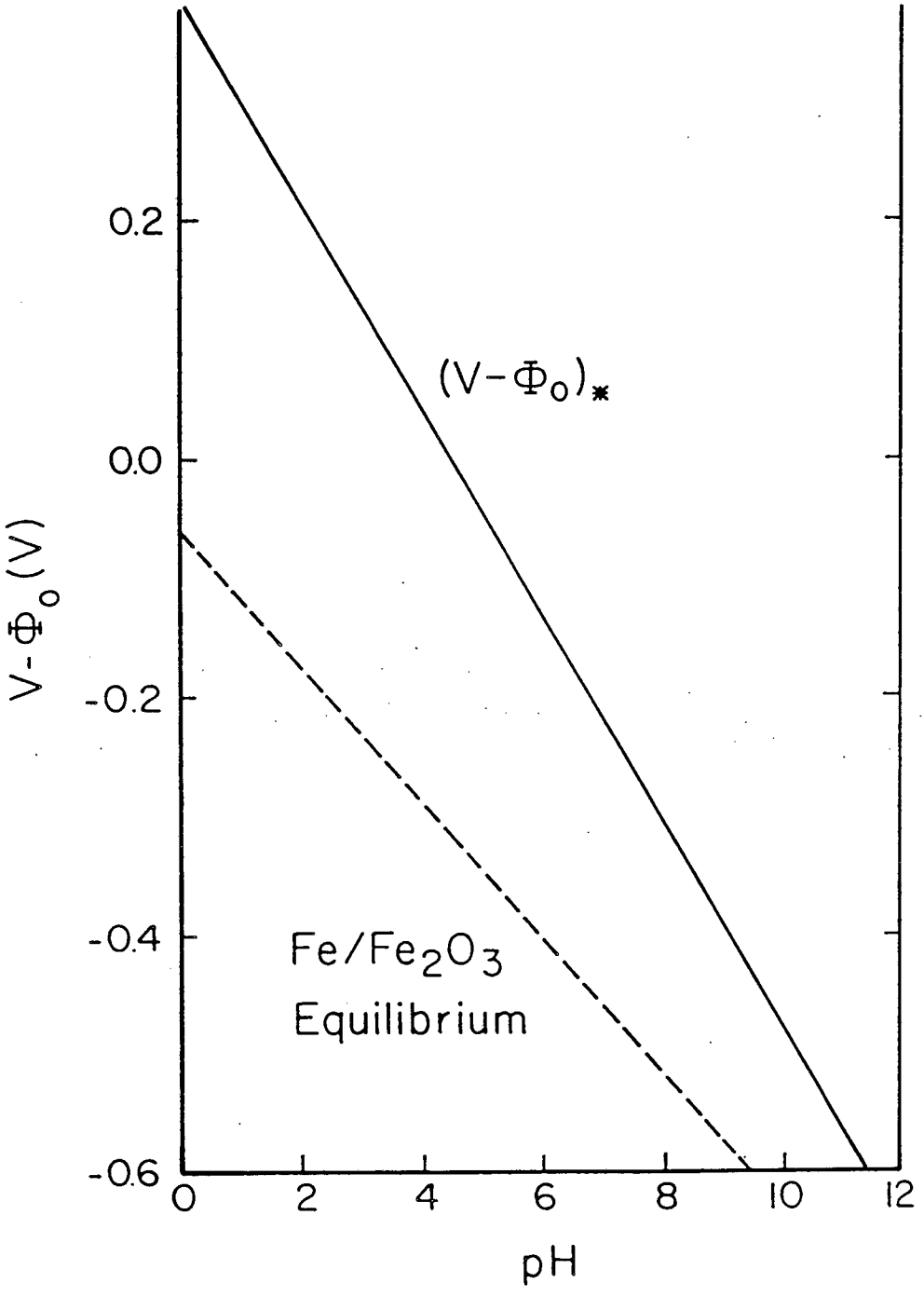

Figure 7. Experimentally determined potential-pH passivation conditions (or Flade potentials) and the theoretical equilibrium between Fe and Fe_2O_3 (dashed line), taken from Pourbaix.[17]

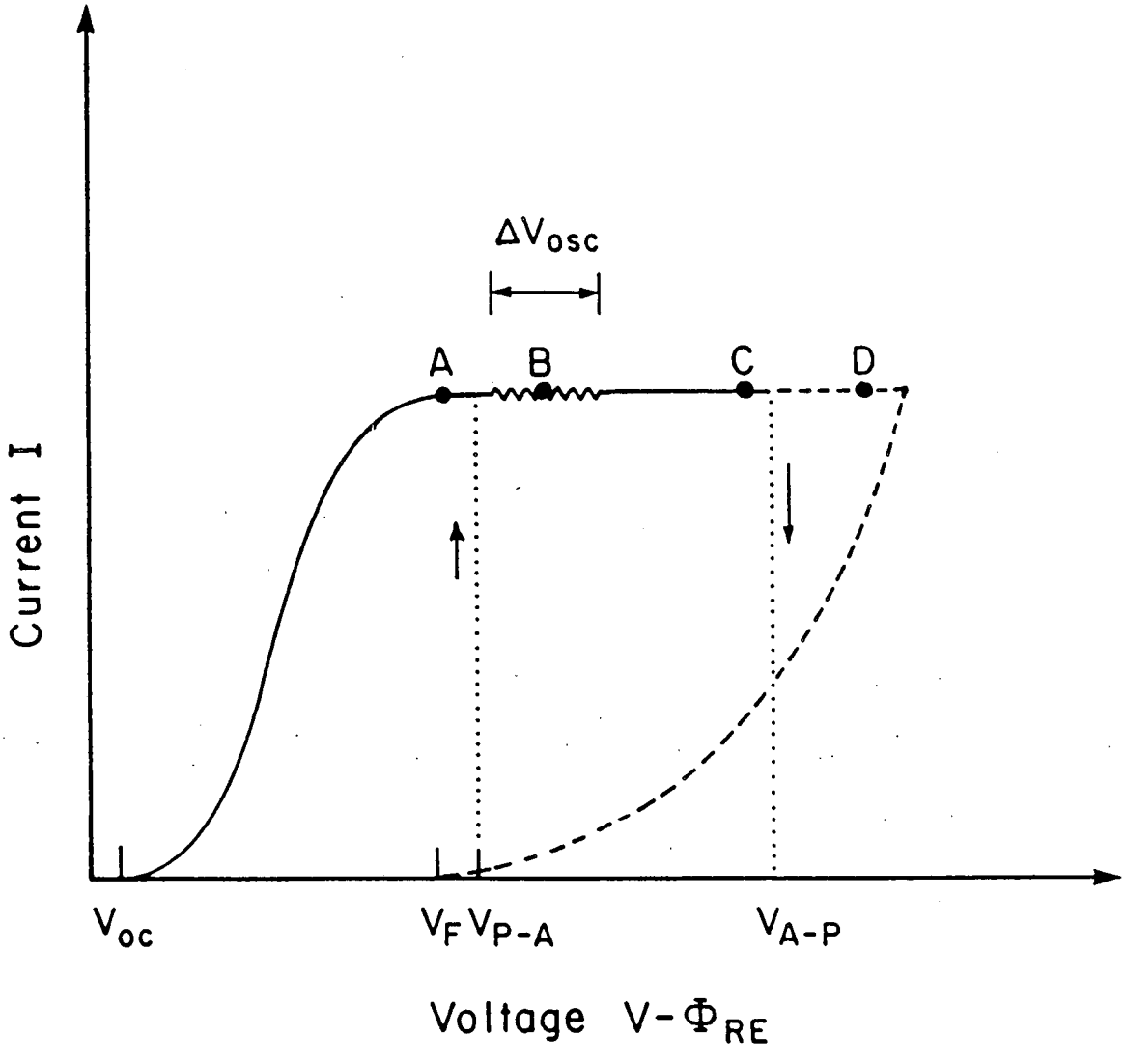

Figure 8. Schematic diagram illustrating a limiting current (due possibly to film formation and dissolution), the potential region where current oscillations are observed, the hysteresis (dotted lines) observed with a normal potentiostat, and the active-passive transition (dashed lines) observable with a potentiostat with a positively sloping load line. Transient overshoot and undershoot phenomena are not included here.

With a normal potentiostat, the electrode would passivate slightly to the right of point C and follow the dotted line down. On the reverse sweep, the electrode would reactivate at V_{P-A} and follow the dotted line upward.

With a potentiostat with a positive-sloping load line,[13] one can follow the dashed active-passive transition coming downward in a curved line beginning to the right of point D. One can think of this as being due to a disk with a shrinking active region near the center and a passive periphery.[10,18] Notice that the potential is relative to the reference electrode in the bulk of the solution and some significant ohmic potential drop is included in the measurement. The Flade potential V_F is also shown on the plot. This would be the passivation potential, in the absence of ohmic potential drop, sketched as the upper line on figure 7.

The behavior to the right of point C can be unstable and show oscillations, but this is sensitive to the potentiostat control settings. There is also an oscillatory region around point B. This is relatively insensitive to the potentiostat settings and can be regarded as being due to the inherent nature of the electrochemical system itself. We have studied this in more detail.[19,21,22] Figure 9 shows that the current can oscillate between a minimum and a maximum which is three times larger than the minimum. At the maximum, most of the disk electrode surface should be active. At the minimum, there must still be an active center region since the current has not dropped to zero, but the outer region of the disk electrode should now

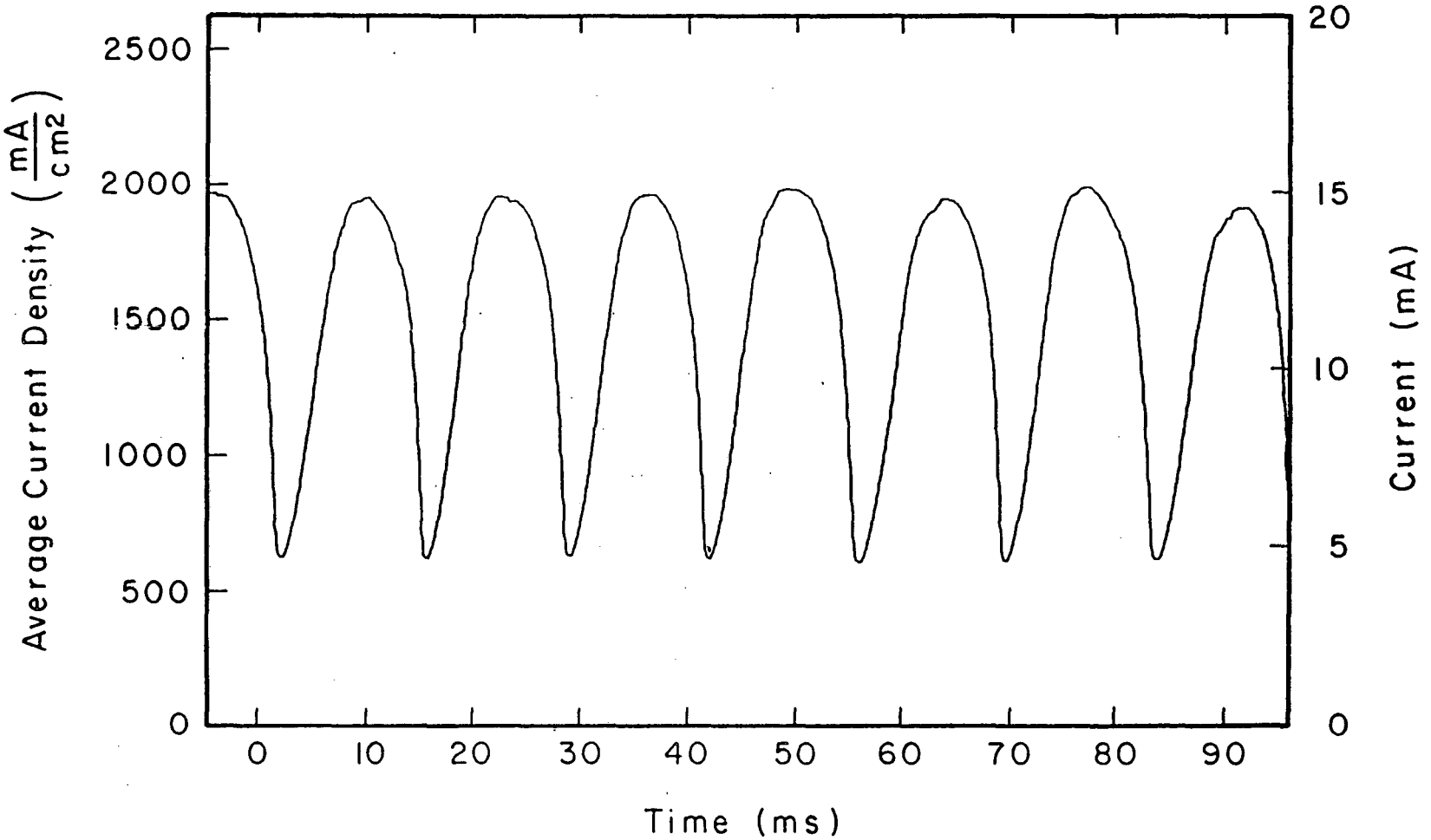

Figure 9. A uniform oscillatory pattern observed for an iron disk of radius=0.0986 cm rotating at 377.0 rad/s in 1 M H_2SO_4 electrolytic solution and potentiostated at -0.271 V relative to a distant mercury-mercurous sulfate reference electrode.

be passivated.

Figure 9 shows some of the cleaner, prettier oscillations that we have observed. One can also see oscillations where a shoulder grows on a wave and a subharmonic oscillation develops.[19,21] Often one sees noise near the minimum of an oscillation. A faster oscilloscope speed reveals that these are oscillations at a higher frequency.[19,21]

It would be interesting to have a detailed model showing quantitatively how salt-film formation, concentration variations, and ohmic potential drop can interact to produce such oscillations. Figure 10 shows on a Pourbaix diagram how such oscillations can occur. These are the result of model calculations.[21,22] Three separate sets are illustrated, corresponding to different parameter values. Let us ignore the set labeled (b), near a pH of 3.3. At (a), two nearly identical sets are labeled (i) and (ii). We need to discuss only set (i). Here the electrode is potentiostated, relative to a reference electrode in the bulk solution, but the ohmic potential drop between these electrodes implies that the ordinate on the Pourbaix diagram can change as the current and compositions change. In all cases illustrated, there is a porous film of $FeSO_4$ of nearly constant thickness on the electrode. At point 1, the disk is active, and the high current causes hydrogen ions to be driven out of the film. This changes the pH at the electrode surface, under the $FeSO_4$ film. The conductivity and current also change so that the local electrode potential $V - \Phi_0$ rises toward the potentiostated potential. Figure 11 illustrates the composition and potential profile with distance from

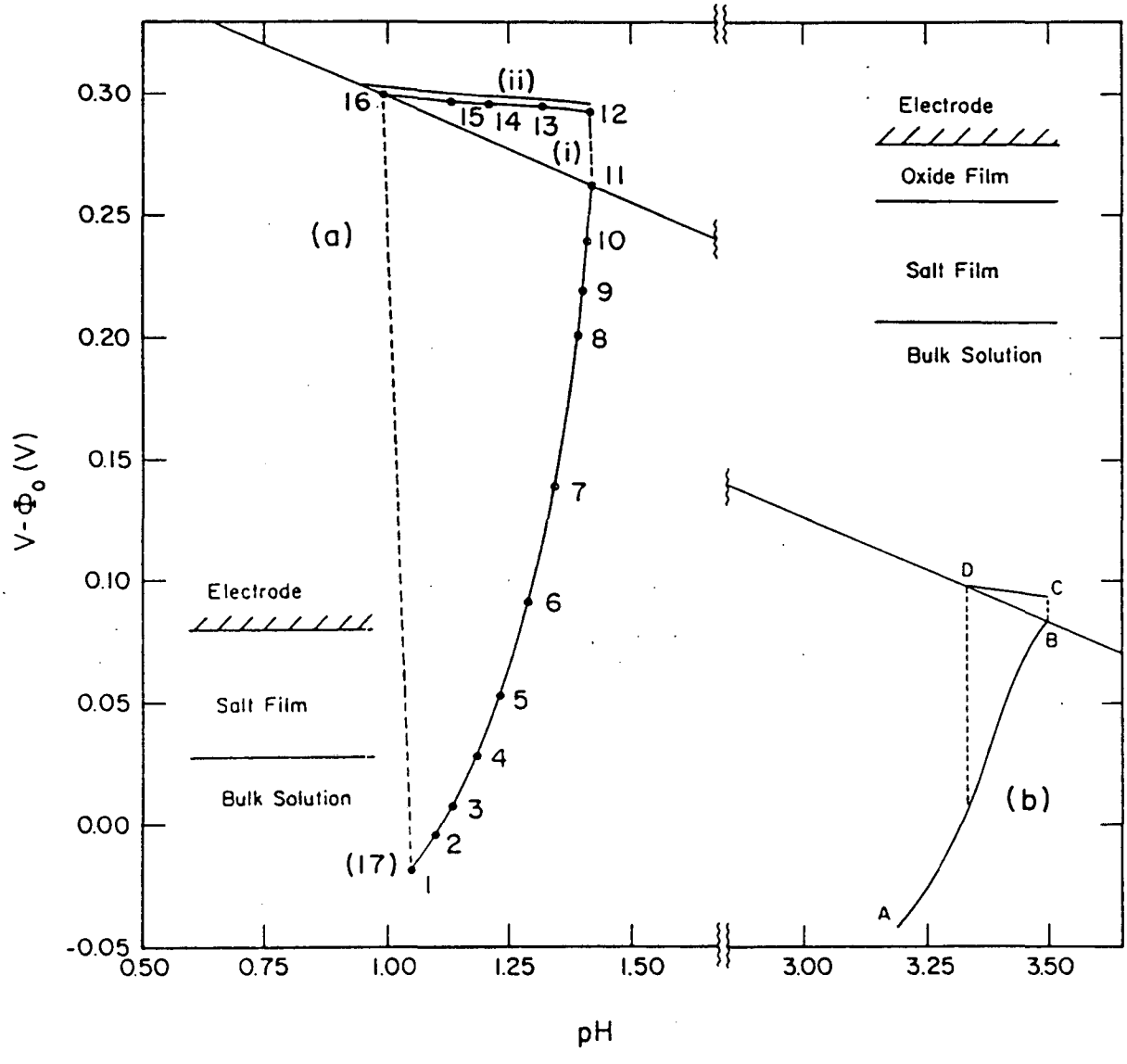

Figure 10. Calculated potential-pH conditions at the electrode surface for three cases.

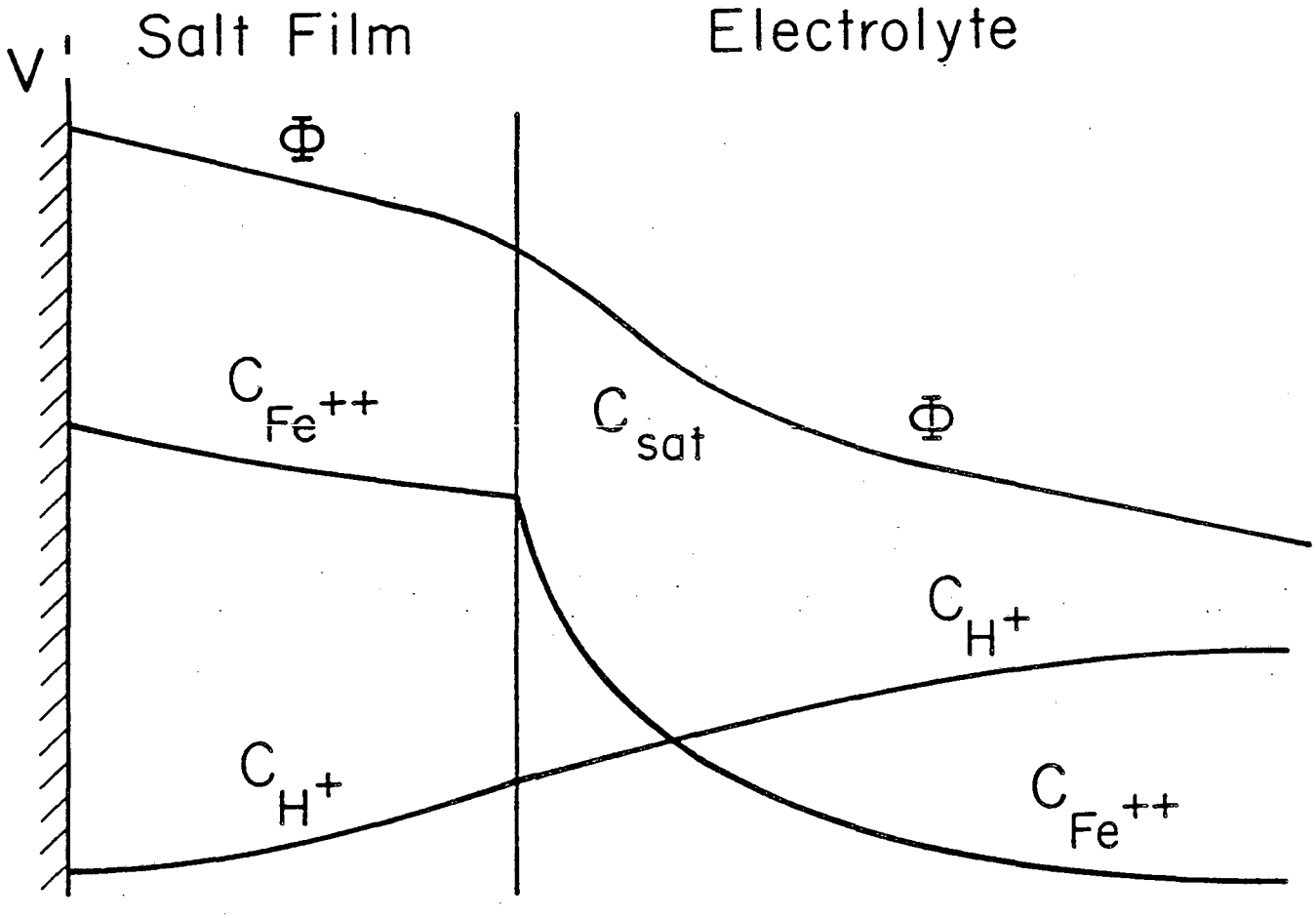

Figure 11. A steep potential gradient is present during active dissolution. Hydrogen ions migrate out of the pores of the salt film, causing a transient increase in pH at the electrode-salt film interface.

the electrode, through the film and out into the solution.

At point 11 on figure 10, the electrode passivates, that is, a thin compact film forms under the salt film. Since the current drops abruptly, the potential rises to point 12 on the Pourbaix diagram. Figure 12 illustrates the concentration and potential profiles. The low electric field allows hydrogen ions to diffuse back into the salt film and lower the pH adjacent to the passivating film. At point 16 on figure 10, the passivation line is again reached, and this time the electrode reactivates and comes to a point (17) close to where it started. Here the current has increased abruptly, and the potential on figure 10 changes sharply, while the compositions, and hence the pH, have no time to change. The oscillatory behavior can now continue. One can see from figure 10, that after passivation at point 11 there is also a strong possibility that the electrode will remain passivated, since it is potentiostated at a relatively high potential and the pH change must be substantial in order to cause reactivation.

The results given here and in the cited references emphasize the importance of a salt film in determining the anodic behavior of iron in the active region and in determining the conditions of passivation. The nature of the oscillations discussed here give insight into the apparently random character of localized corrosion. The condition of a partly active, partly passive surface is not easy to predict and can be physically unstable.

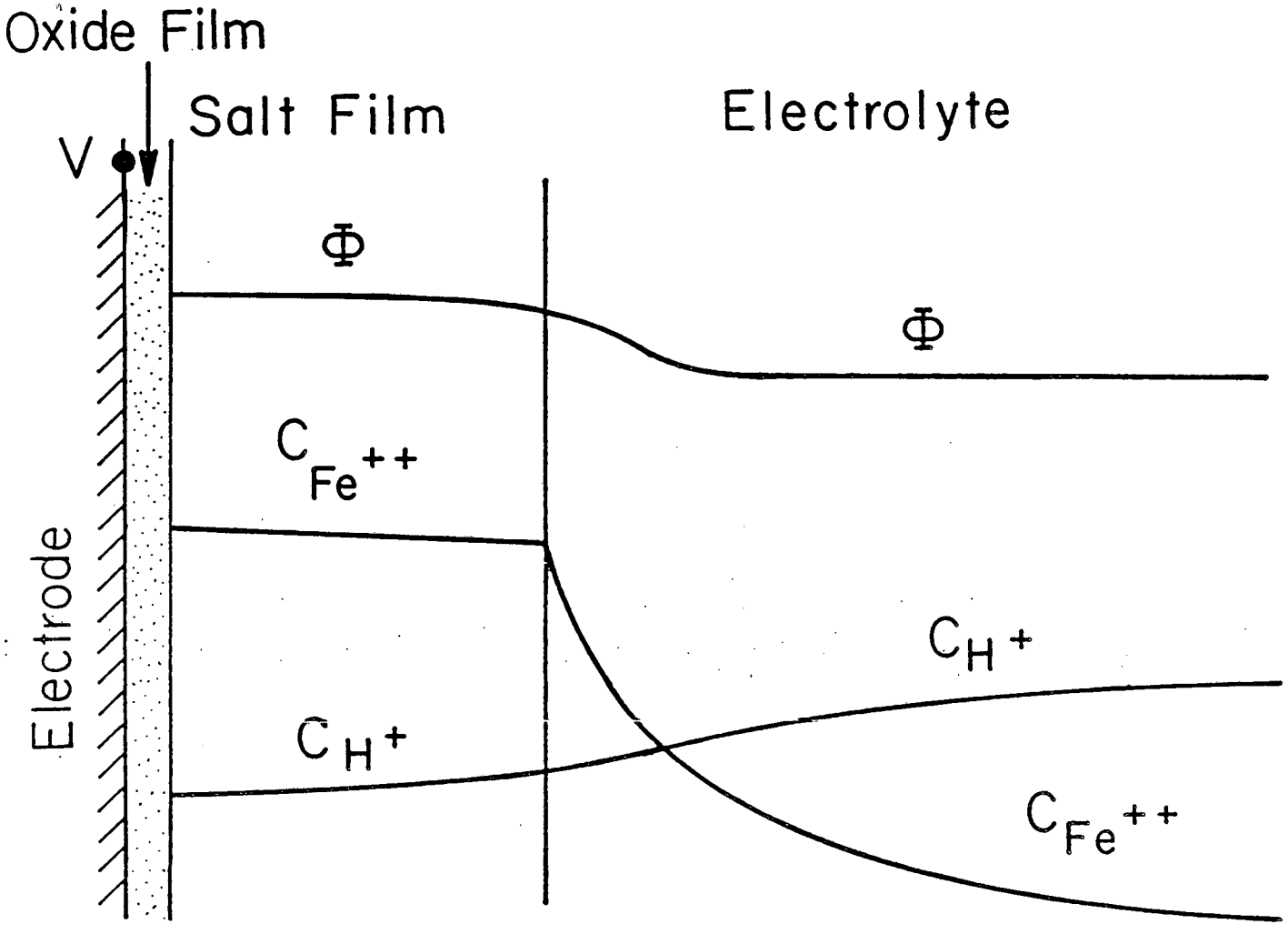

Passive State

Figure 12. When the electrode is passivated, hydrogen ions diffuse back into the pores of the salt film because the electric field is substantially reduced.

Corrosion of Iron in Sea Water

Some years ago, LaQue[23,24] showed fascinating results for the corrosion of rotating disks in sea water. The copper disks corroded preferentially near the periphery, while the iron disks corroded preferentially near the center and were passivated near the edge. This seemed like an excellent system for developing a model of localized corrosion,[2] one where hydrodynamics were known or could be described and for which methods had been worked out for treating both potential distributions and mass transfer.[6] The concept was that turbulent flow, and therefore enhanced mass transfer of oxygen, occurred near the periphery of the disks, and this resulted in increased corrosion in the case of copper and to passivation in the case of iron. In the absence of the experimental results of LaQue, one might have assumed that a situation of a partly active and a partly passive disk would have been unstable.

Again, it is desirable to see how well a quantitative model of mass transfer, potential distribution, and passivation can reproduce the results already obtained experimentally and to see how parameters such as oxygen concentration, disk radius, rotation speed, and solution conductivity affect the results.

Vahdat and Newman[25] reported results of modeling efforts in 1973. Since then, we have used a more realistic passivation curve, and we have studied the hydrodynamics and mass transfer in more detail for the disk geometry. Von Kármán[26] studied the hydrodynamics. The center of the disk involves laminar flow, for which Levich[27] has

showed us how to treat the mass transfer. This region turns out to be "uniformly accessible" from a mass-transfer standpoint—that is, the limiting-current distribution is uniform in this region.

Mohr and Newman[28] measured limiting rates of mass transfer for disks in the transition region and showed how to infer the local rate of mass transfer from the overall rate. They augmented their experimental results with those of Daguenet[29] and gave expressions for this local rate of mass transfer in the transition and fully-developed turbulent regions, in addition to that in the laminar region. Because the concentration may vary over the surface of the disk, Law *et al.*[30] used ring electrodes. Supplementing their experimental results with those of Deslouis and Keddam[31] on rings and the previous authors on disks, they developed a procedure for calculating limiting mass-transfer rates to disk and ring electrodes with flow regimes including the laminar, transitional, and fully turbulent. This procedure was extended by Law and Newman[11] to cover electrodes with variable surface concentration by means of a superposition integral.

Law and Newman[11] refined the model of Vahdat and Newman to include our best understanding of passivation and mass transfer. Figure 13 compares the experimental results of LaQue with the model results for the radius of passivation for three overall disk radii. We are pleased with the agreement, although it is not perfect.

Figure 14 gives a more detailed view of the complex processes. As functions of radial position, one sees the local current densities for the oxygen-reduction and iron-dissolution reactions and the

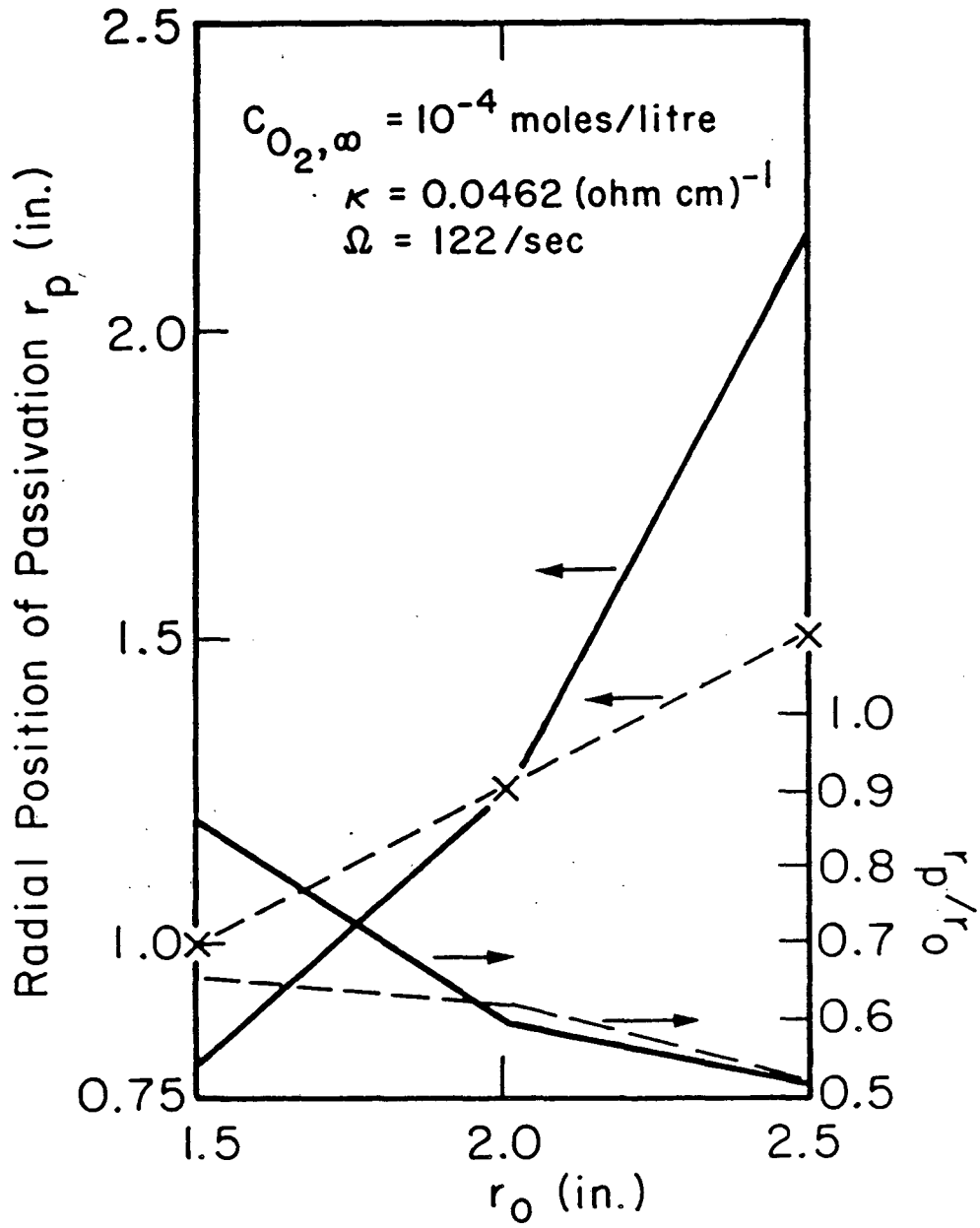

Figure 13. Comparison of the measured (---) (LaQue[23]) and calculated (——) (Law and Newman[11]) radii of passivation for iron disks rotating in sea water.

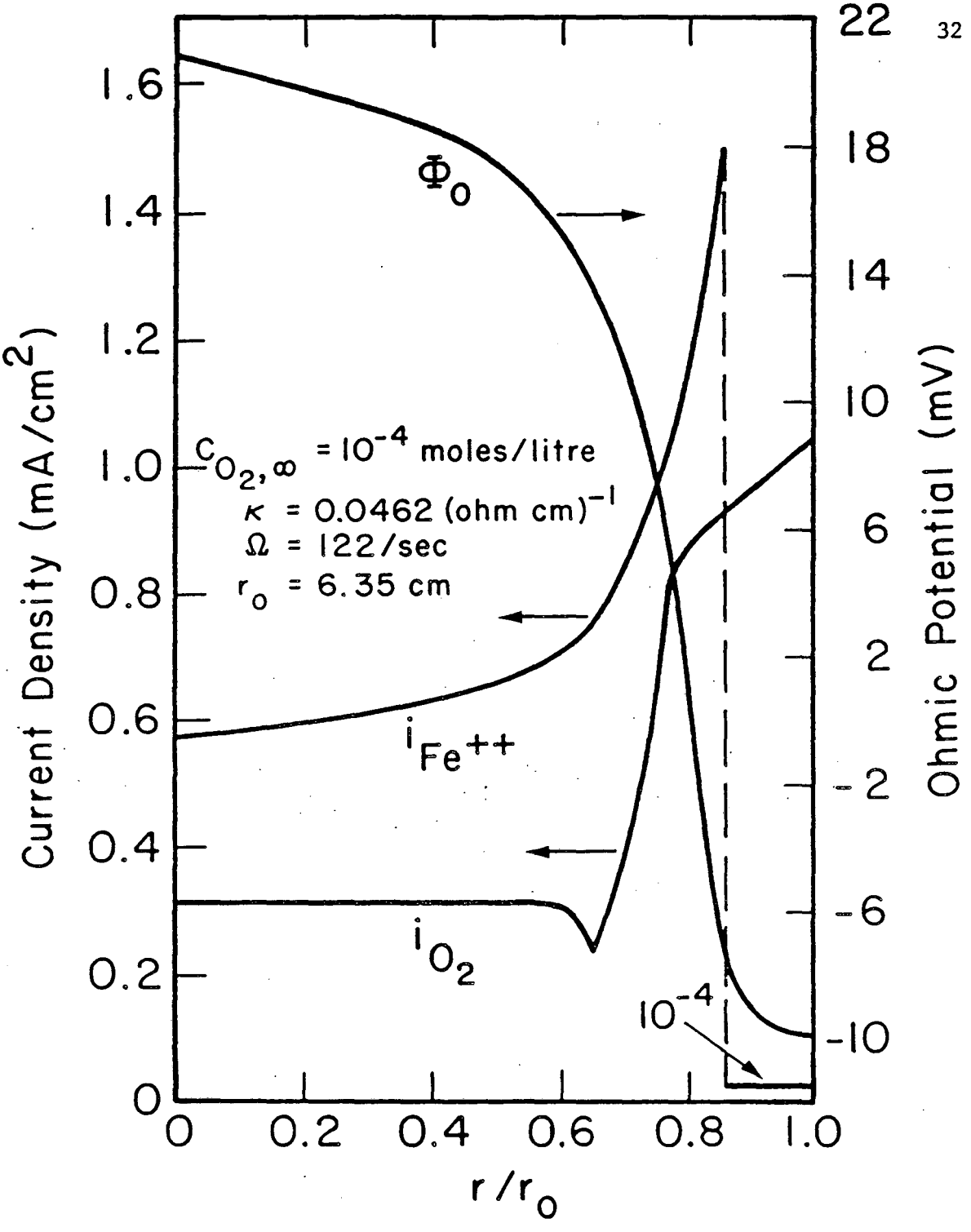

Figure 14. Current and potential distributions, calculated for oxygen-corrosion of an iron disk rotating in sea water.

potential Φ_0 in the solution adjacent to the surface. Because the equilibrium potential for the oxygen reaction is quite positive, the oxygen reaction is found to be at the limiting current under the conditions depicted here. Thus, near the center of the disk, where the flow is laminar, the oxygen transport is uniform and given by the Levich formula. The transition region extends from $r/r_0 = 0.6$ to about 0.75. Here the mass-transfer rate is actually expected to decrease, as shown in the figure, before it begins to increase. The fully-developed turbulent-flow region begins at about 0.75.

The curve for the current density of iron dissolution shows the calculated value to increase from the center, but at the radius of passivation (r/r_0 equal to about 0.85) the current density drops sharply. This would correspond to the point where $V - \Phi_0$ equals the value given by the Pourbaix criterion for passivation at this pH (see figure 7 or a source specific to sea water). The potential distribution Φ_0 decreases from the center toward the periphery because the anodic process dominates near the center while the cathodic process dominates near the edge (compare figure 4).

The total oxygen current must balance the total iron current on figure 14, as this is the condition for corrosion. It is not always possible for the iron dissolution to keep pace with the limiting rate of transport of oxygen to the surface, and then it will not be possible to maintain the disk in a partly active, partly passive condition. The entire disk will passivate. Figure 15 illustrates, from the calculations, how large values of the disk rotation speed or of the disk

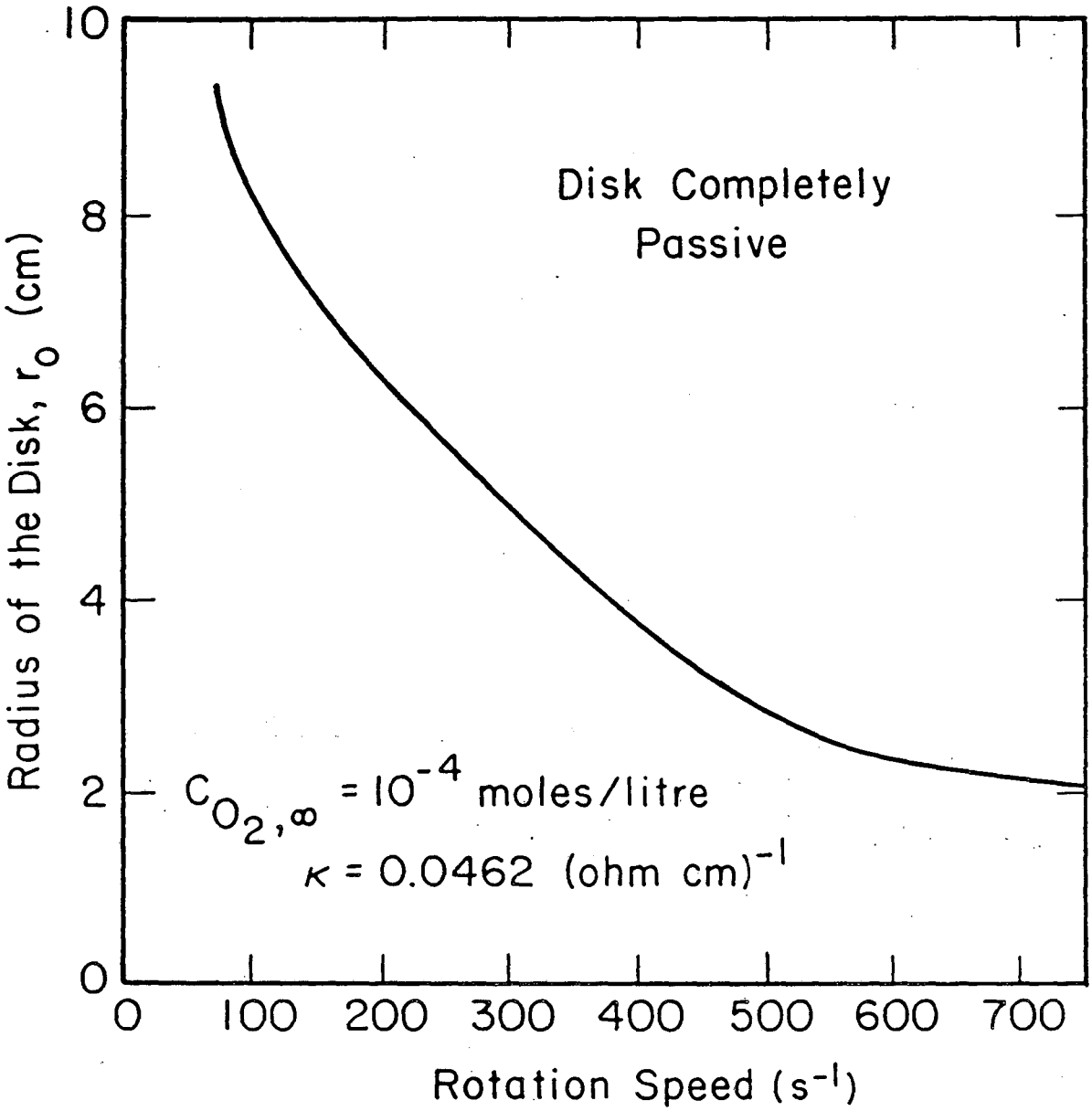

Figure 15. Envelope indicating region of passivity. Partly active, partly passive behavior should not occur above the solid curve.

radius would be expected to lead to complete passivation. Other parameters, such as bulk oxygen concentration and solution conductivity would also have an effect, which is not shown on this figure. Conductivity is a particularly interesting parameter for localized corrosion. At very low conductivities, the solution would behave as an insulator, and current could not flow from one region to another. At very high conductivities, the electrochemical cell would be shorted, and one might expect completely passive or completely active behavior. Only at intermediate values of the conductivity would one expect localized corrosion, where the anodic and cathodic reactions occur, more or less, on different parts of the surface.

Conclusions

While localized corrosion is an interesting process, requiring a passivating reaction, it can lead to catastrophic failure by concentrating the corrosive tendency of cathodic processes into intensive anodic dissolution in a small locality.

Localized corrosion is complex because it involves current flow within the solution and substantial concentration variations. Research in this area requires refinement of our knowledge of passivation and the development of mathematical models dealing with these phenomena and salt-film formation. The rotating disk is an attractive research tool because hydrodynamics, potential distributions, and mass transfer are reasonably well understood for this system.

Acknowledgment

This work was supported by the Assistant Secretary for Conservation and Renewable Energy, Office of Energy Systems Research, Energy Storage Division of the U. S. Department of Energy under Contract No. DE-AC03-76SF00098.

List of Symbols

c_i	concentration of species i, mol/cm^3
D_i	diffusion coefficient of species i, cm^2/s
F	Faraday's constant, 96487 C/equiv
i	current density, A/cm^2
N_i	flux density of species i, $mol/cm^2 \cdot s$
r	radial position, cm
r_0	radius of pit, disk, or hemisphere, cm
R_i	rate of production of species i by homogeneous chemical reactions, $mol/cm^3 \cdot s$
t	time, s
u_i	mobility of species i, $cm^2 \cdot mol/J \cdot s$
v	fluid velocity, cm/s
V	potential for metal, V
z_i	charge number of species i

Greek letters

κ	conductivity of solution, mho/cm
Φ	potential of solution, V

References

1. John S. Newman. *Electrochemical Systems*. Englewood Cliffs, N. J.: Prentice-Hall, Inc., 1973.

2. John Newman. "Mass Transport and Potential Distribution in the Geometries of Localized Corrosion." B. F. Brown, J. Kruger, and R. W. Staehle, eds., *Localized Corrosion*, pp. 45-61. Houston: National Association of Corrosion Engineers, 1974.

3. William H. McAdams. *Heat Transmission*, p. 216. New York: McGraw-Hill Book Company, Inc., 1942.

4. John Newman, D. N. Hanson, and K. Vetter. "Potential Distribution in a Corroding Pit." *Electrochimica Acta*," 22 (1977), 829-831.

5. Kemal Nişancioğlu and John Newman. "Current Distribution on a Rotating Sphere below the Limiting Current." *J. Electrochem. Soc.*, 121 (1974), 241-246.

6. John Newman. "Current Distribution on a Rotating Disk below the Limiting Current." *J. Electrochem. Soc.*, 113 (1966), 1235-1241.

7. B. Levich and A. Frumkin. "Ohmic Resistance of Local Cells in the Process of the Solution of Metals in Acids." *Acta Physicochimica U.R.S.S.*, 18 (1943), 325-340.

8. I. Epelboin, C. Gabrielli, M. Keddam, and H. Takenouti. "A Model of the Anodic Behaviour of Iron in Sulphuric Acid Medium." *Electrochim. Acta*, 20 (1975), 913-916.

9. Israël Epelboin, Claude Gabrielli, Michel Keddam, and Hisasi Takenouti. "The Study of the Passivation Process by the Electrode Impedance Analysis." J. O'M. Bockris, Brian E. Conway, Ernest Yeager, and Ralph E. White, eds. *Comprehensive Treatise of Electrochemistry*, 4, 151-192. New York: Plenum Press, 1981.

10. Clarence G. Law, Jr., and John Newman. "A Model for the Anodic Dissolution of Iron in Sulfuric Acid." *J. Electrochem. Soc.*, 126 (1979), 2150-2155.

11. Clarence G. Law, Jr., and John Newman. "Corrosion of a Rotating Iron Disk in Laminar, Transition, and Fully Developed Turbulent Flow." *J. Electrochem. Soc.*, 133 (1986), 37-42.

12. A. A. El Miligy, D. Geana, and W. J. Lorenz. "A Theoretical Treatment of the Kinetics of Iron Dissolution and Passivation." *Electrochim. Acta*, 20 (1975), 273-281.

13. Israël Epelboin, Claude Gabrielli, Michel Keddam, Jean-Claude Lestrade, and Hisasi Takenouti. "Passivation of Iron in Sulfuric Acid Medium." *J. Electrochem. Soc.*, 119 (1972), 1632-1637.

14. K. J. Vetter and H. H. Strehblow. "Pitting Corrosion in an Early Stage and Its Theoretical Implications." B. F. Brown, J. Kruger, and R. W. Staehle, eds., *Localized Corrosion*, pp. 240-251. Houston: National Association of Corrosion Engineers, 1974.

15. Richard Alkire, Daniel Ernsberger, and Theodore R. Beck. "Occurrence of Salt Films during Repassivation of Newly Generated Metal Surfaces." *J. Electrochem. Soc.*, 125 (1978), 1382-1388.

16. Theodore R. Beck. "Occurrence and Properties of Anodic Salt Films in Localized Corrosion." *International Conference on Localized Corrosion*. Orlando, Florida. National Association of Corrosion Engineers, June 1, 1987.

17. Marcel Pourbaix. *Atlas of Electrochemical Equilibria in Aqueous Solutions*. Houston: National Association of Corrosion Engineers, 1974.

18. Philip P. Russell and John Newman. "Experimental Determination of the Passive-Active Transition for Iron in 1 M Sulfuric Acid." *J. Electrochem. Soc.*, 130 (1983), 547-553.

19. Philip Russell and John Newman. "Current Oscillations Observed within the Limiting Current Plateau for Iron in Sulfuric Acid." *J. Electrochem. Soc.*, 133 (1986), 2093-2097.

20. Theodore R. Beck. "Formation of Salt Films during Passivation of Iron." *J. Electrochem. Soc.*, 129 (1982), 2412-2418.

21. Philip Paul Russell. *Corrosion of Iron: The Active-Passive Transition and Sustained Electrochemical Oscillations*. Dissertation. Berkeley: University of California, 1984.

22. Philip Russell and John Newman. "Anodic Dissolution of Iron in Acidic Sulfate Electrolytes. II. Mathematical Model of Current Oscillations Observed under Potentiostatic Conditions." *J. Electrochem. Soc.*, 134 (1987), 1051-1059.

23. F. L. LaQue. "Theoretical Studies and Laboratory Techniques in Sea Water Corrosion Testing Evaluation." *Corrosion*, 13 (1957),

303t-314t.

24. F. L. LaQue. "Electrochemistry and Corrosion (Research and Tests)." *J. Electrochem. Soc.*, 116 (1969), 73C-77C.

25. Nader Vahdat and John Newman. "Corrosion of an Iron Rotating Disk." *J. Electrochem. Soc.*, 120 (1973), 1682-1686.

26. Th. v. Kármán. "Über laminare und turbulente Reibung." *Z. angew. Math. Mech.*, 1 (1921), 233-252.

27. B. Levich. "The Theory of Concentration Polarization." *Acta Physicochimica U.R.S.S.*, 17 (1942), 257-307.

28. Charles M. Mohr, Jr., and John Newman. "Mass Transfer to a Rotating Disk in Transition Flow." *J. Electrochem. Soc.*, 123 (1976), 1687-1691.

29. Michel Daguenet. "Etude du transport de matière en solution, à l'aide des électrodes à disque et à anneau tournant." *Int. J. Heat Mass Transfer*, 11 (1968), 1581-1596.

30. Clarence G. Law, Jr., Peter Pierini, and John Newman. "Mass Transfer to Rotating Disks and Rotating Rings in Laminar, Transition and Fully-Developed Turbulent Flow." *Int. J. Heat Mass Transfer*, 24 (1981), 909-918.

31. C. Deslouis and M. Keddam. "Emploi d'électrodes à anneau tournant à l'étude du transport de matière dans un fluide en régime hydrodynamique laminaire ou turbulent." *Int. J. Heat Mass Transfer*, 16 (1973), 1763-1775.

LAWRENCE BERKELEY LABORATORY
TECHNICAL INFORMATION DEPARTMENT
UNIVERSITY OF CALIFORNIA
BERKELEY, CALIFORNIA 94720